REGULATION OF EPIDERMAL CELL

PRODUCTION BY THE *SUPPRESSOR OF ERECTA*

AND *ERECTA* GENES IN *ARABIDOPSIS THALIANA*

By

XI WEN

Bachelor of Science in Agriculture

Shandong Agricultural University

Tai'an, China

2018

Submitted to the Faculty of the
Graduate College of the
Oklahoma State University
in partial fulfillment of
the requirements for
the Degree of
MASTER OF SCIENCE
December, 2021

REGULATION OF EPIDERMAL CELL

PRODUCTION BY THE *SUPPRESSOR OF ERECTA*

AND *ERECTA* GENES IN *ARABIDOPSIS THALIANA*

Thesis Approved:

Dr. Ming Yang

Thesis Adviser

Dr. Andrew Doust

Dr. Heejin Yoo

Name: XI WEN

Date of Degree: DECEMBER 2021

Title of Study: REGULATION OF EPIDERMAL CELL PRODUCTION BY THE *SUPPRESSOR OF ERECTA* AND *ERECTA* GENES IN *ARABIDOPSIS THALIANA*

Major Field: PLANT BIOLOGY

Abstract: Despite many scientific studies on plant epidermal cell development and differentiation, the knowledge on molecular regulation of the ontogeny of plant epidermal cells is still very limited. The biggest breakthrough is the establishment of signaling pathways for stomatal lineage formation in Arabidopsis, which start from extracellular signaling peptides to their transmembrane receptor kinase complexes to mitogen-activated protein kinase (MAPK) cascades and eventually to transcription factors. Several leucine-rich repeat receptor kinases (LRR-RKs), including the ERECTA (ER) protein, are known to be involved in this signaling process. ER regulates stomatal patterning and proliferation of epidermal cells. To identify additional mutations affecting epidermal cell production in the ecotype of Landsberg *erecta* (Ler, containing the *er-1* mutation), our lab looked for DNA polymorphisms that were linked to the Ler-like epidermal phenotype in the F_2 progeny of a cross between Ler and Col-0 (wild type). We identified a deletion of two adjacent LRR-RKs in a region of approximately 21kb on chromosome 2 in Ler that may be involved in epidermal cell production. My thesis research primarily focused on the functional characterization of this deleted region and one of the candidate genes, At2G29000. I found that mutations of At2G29000 partially suppressed the increased epidermal cell phenotype of *er* mutants, which were thus named *suppressor of erecta* (*sue*). The heterozygous *er-1* mutation together with a heterozygous *sue-1* mutation also resulted in a Ler-like epidermal phenotype. The suppression of *sue* on *er* is stronger on the adaxial epidermis than on the abaxial epidermis, which seemed to correlate with the stronger *SUE* expression in the adaxial epidermis than in the abaxial epidermis based on GUS-reporter gene studies for *SUE*. The interaction between *sue* and *erecta* on epidermal cell production was neither additive nor epistatic and the outcomes suggested a dosage effect between them. Both the *sue* and *er* mutations were found to suppress trichome production. The phenotypic and genotypic results suggested that the other candidate gene At2G28990 also played a role similar to that of *SUE* in the regulation of epidermal cell production. This research has provided evidence that two novel LRR-RK genes regulate epidermal development, and novel observations of the effect of *er* mutations on epidermal cell production.

TABLE OF CONTENTS

LIST OF TABLES

LIST OF FIGURES

CHAPTER I

INTRODUCTION

Stomata and their functions

A stoma is a microscopic pore flanked by two guard cells in the above-ground epidermis of plants. With the ability to close or open the pore in response to environmental signals, stomata serve as valves for gas exchange between internal tissues of a plant and the atmosphere (Hetherington & Woodward, 2003). In addition, plant transpiration occurs mostly through open stomata that only take up approximately 5% of leaf area (Willmer, 1996). Both gas exchange and transpiration are crucial to plant growth and development. As the most important structure for regulating air exchange, stomatal movement has been found to respond to abscisic acid, CO_2 concentration, blue and red light (Kollist *et al*., 2014).

Facing long-term and/or short-term climate changes, some parts of the world are expected to experience drought (Bertolino *et al*., 2019). A drought-tolerant species may have a smaller value of water use efficiency (WUE), defined by the ratio of the amount of water used to the amount of biomass gained, than a drought-intolerant species. Naturally, the value of WUE should be significantly correlated with stomatal density and dynamics in stomatal pore size regulation. Several genes are found to affect WUE by regulating stomata development and movement. *STOMATAL DENSITY AND DISTRIBUTION1 (SDD1)*, which is strongly expressed in stomatal precursor cells, encodes a subtilisin-like serine protease. The mutation of *SDD1* leads to clustering of stomata and up to twofold to fourfold stomatal density increase (von Groll *et al*., 2002). Interestingly, the transcription factor GT-2 LIKE 1 (GTL1) negatively regulates the expression of *SDD1*, and a loss-of-function mutation of *GTL1* resulted in smaller WUE values by reducing abaxial stomatal density (Yoo *et al*., 2010). In this case, CO_2 assimilation was not obviously compromised while a 25% reduction in transpiration and stomatal conductance were estimated. Another drought tolerance gene, *HDG11*, which encodes a protein in the homeodomain-START

transcription factor family, functions in reducing leaf stomatal density and increasing primary root growth and later root number (Yu *et al*., 2008). Moreover, an antisense line of the calcium-sensing receptor CAS, which is considered the primary transducer of Ca^{2+} signaling in plants (Han *et al.*, 2003), was found to improperly regulate stomatal pore closure under drought condition and reduce CO_2 assimilation rate, leading to decreased WUE (Wang *et al*., 2013).

<div align="center">Stomatal lineage development and regulation</div>

In plants, the number of stomata is developmentally regulated, setting the upper and lower thresholds of gas exchange (Hetherington & Woodward, 2003).
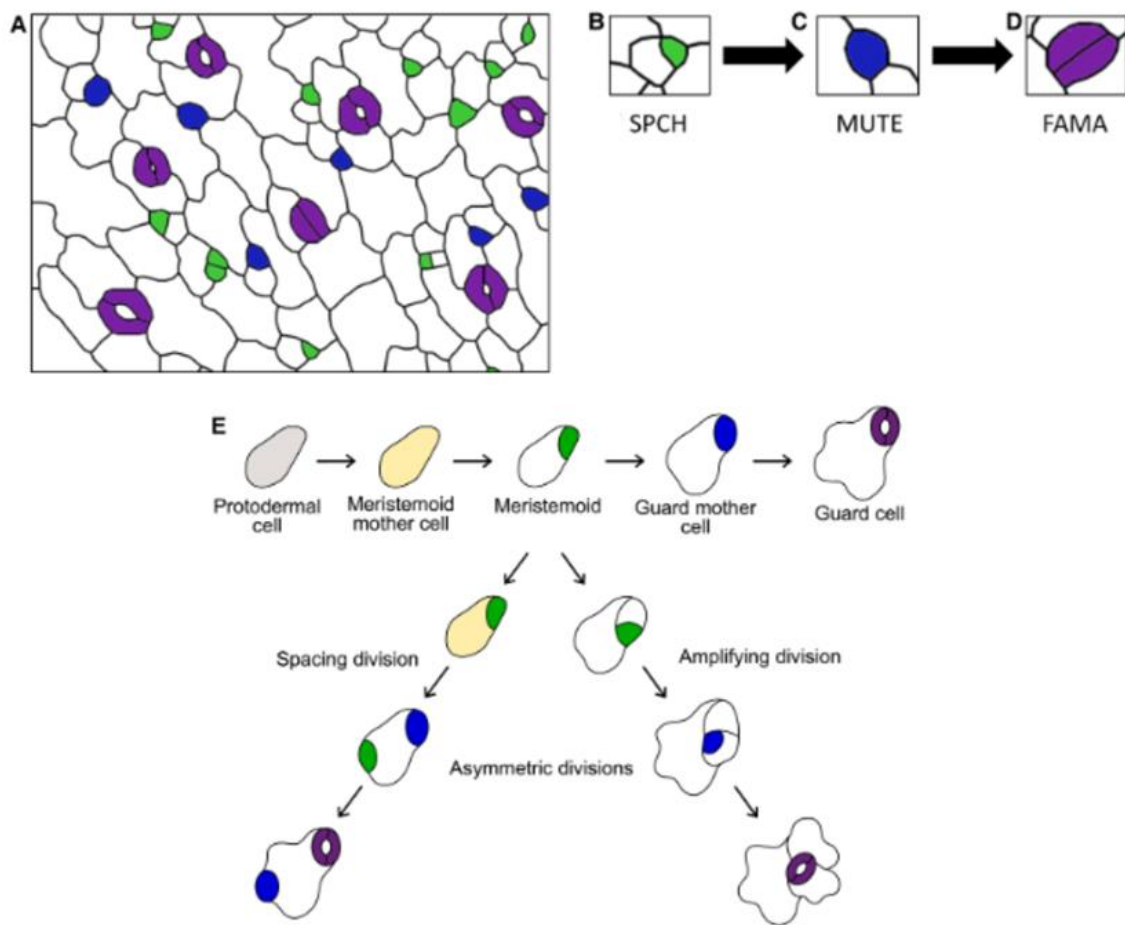
Fig. 1. Schematic illustration of stomatal lineage formation and its transcriptional regulation (Zoulias *et al*., 2018). **A**. Young abaxial epidermis showing the expression of three bHLH transcription factors, SPCH, MUTE, and FAMA, in various stages of stomatal development. **B**. MMC or meristemoid contains SPCH (green). **C**. GMC contains MUTE (blue). **D**. Maturing guard cells contain FAMA (purple). **E**. Three modes of stomatal lineage formation.

A stomatal lineage in the epidermis starts from a protodermal cell that divides to produce meristemoid mother cells (MMC) (**Fig. 1E**). An MMC then undergoes an asymmetric division to produce a smaller meristemoid and a larger cell. The larger cell may become a stomatal linage ground cell (SLGC, or pavement cell) and the meristemoid a guard mother cell. Alternatively, the larger cell may continue to divide (spacing division) to produce another meristemoid that also turns into a GMC; the two meristemoids are separated by a SLGC. Still a third possible scenario is that the meristemoid from the MMC divides one or more times (amplifying divisions) to produce one or more SLGCs and a terminal GMC. In all the scenarios, the GMC divides one last time to produce two guard cells (Geisler *et al*., 2000; Larkin *et al*., 1997; Lucas *et al*., 2005).

Formation of the different cell types in the stomatal lineage is regulated by three homologous basic helix-loop-helix (bHLH) transcription factors, SPEECHLESS (SPCH), MUTE, and FAMA. SPCH is required for the formation of the meristemoid mother cell and its asymmetric division (MacAlister *et al*., 2007).

Fig. 2. Signaling pathway of stomatal development controlled by SPCH in Arabidopsis. The diagram illustrates the signaling pathway from the extracellular peptides EPF1/2 or STOMAGEN to the transcription factor SPCH in the nucleus. EPF1/2 and STOMAGEN competes to bind with the membrane complex forme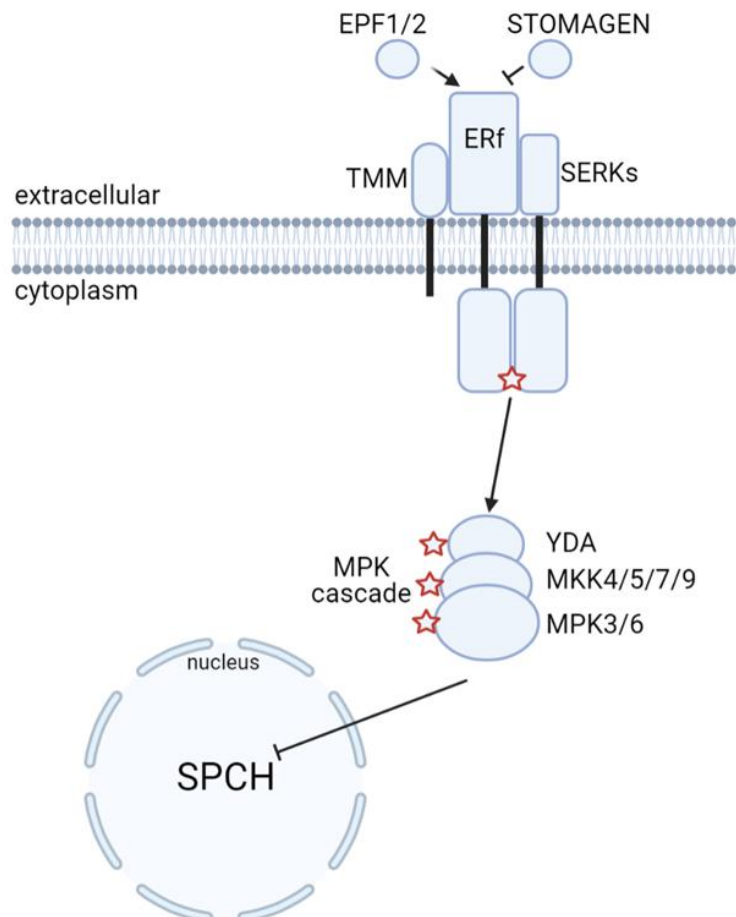d by TMM, ERf and SERKs. The intracellular kinase domains of ERf and SERKs conduct phosphorylation to start the MPK cascade. Through this cascade, the signal will be transmitted to SPCH to induce stomatal development. Arrow lines indicate positive regulation. Bar lines indicate negative regulation. Red asterisks represent phosphorylation. This illustrative figure is accomplished in biorender (https://app.biorender.com/).

MUTE regulates the transition from the meristemoid to the guard mother cell; whose loss-of-function mutants fail to differentiate stomata (Pillitteri *et al*., 2007). FAMA regulates the final symmetrical division of the GMC for guard cell production (Ohashi-Ito & Bergmann, 2006). Together, SPCH, MUTE and FAMA transcriptionally regulate the entire process of stomatal lineage formation.

Leucine-rich repeat receptor kinases (LRR-RKs) are the largest family of transmembrane receptor-like kinases in Arabidopsis with more than 200 members (Torii *et al*., 2004). As one of the most well studied subfamilies of the LRR-RK family, the ERECTA subfamily (ERf) consists of *ERECTA* (*ER*) and its two paralogues *ERECTA-LIKE1* (*ERL1*)and *ERECTA-LIKE2* (*ERL2*) (Shpak *et al*., 2004). ERf plays critical roles in stomatal lineage formation (**Fig. 2**). LRR-RKs usually form a complex by themselves and with leucine-rich repeat receptor-like proteins (LRR-RLPs) (Zoulias *et al*., 2018). Different combinations of these proteins enable the complexes to interact with different signaling molecules. One of the most important and the first characterized LRR-RLP is *TOO MANY MOUTHS* (*TMM*), which regulates the development of stomatal lineage. Several secreted peptides such as EPF1 (Hara *et al*., 2007), EPF2 (Hunt & Gray, 2009), EPFL9 (Hunt *et al*., 2010) and STOMAGEN (Sugano *et al*., 2010) have been found to interact with cell membrane receptors to regulate stomatal development. TMM binds to ER and ERL1 to form a membrane receptor complex for the negative stomatal lineage regulators EPF1 and EPF2 (Lee *et al*., 2012). A *tmm* mutant contains increased and clustered stomata, increased meristemoids, and reduced pavement cells (Yang & Sack, 1995; Geisler *et al*., 2000). The stomatal lineage positive regulator STOMAGEN also signals through TMM and ER/ERL1/ERL2, which competes with EPF1 and EPF2 for binding to the receptor complex(Lee *et al*., 2015).

As the membrane receptor of brassinosteriods, BRASSINOSTERIOD INSENSITIVE1 (BRI1) function together with brassinosteriods in the development of epidermal cells. Stomatal clusters were discovered in *bri1* mutants in Arabidopsis cotyledons, and stomatal density were reduced when applied brassinolide (Kim *et al.*, 2012). BRI1-associated

receptor kinase (BAK1) was identified as the signaling regulator of BRI1 (Li *et al.*, 2002), and BAK1 is also known as SOMATIC EMBRYOGENESIS RECEPTOR KINASE3 (SERK3) (aan den Toorn *et al.*, 2015). The family of somatic embryogenesis receptor kinases (SERKs) with a characteristic serine-proline-rich region can interact with TMM and the ERf members (Meng *et al.*, 2015). SERKs are redundant in stomatal patterning regulation as suggested by the phenotypic analysis of single, double, and triple mutants of *serk1-1, serk2-1, and bak1-4* (Meng *et al.*, 2015). Four SERKs contribute unequally to stomatal patterning with descending order of importance from SERK3 to SERK2 to SERK1 to SERK4 (Meng *et al.*, 2015).

The intermediate signaling components linking the ERf/TMM/SERK complexes to the transcription factors are those of the intracellular mitogen-activated protein kinase (MAPK) pathway (**Fig. 2**). The signaling cascade starts from binding of the extracellular peptides EPF1/2 and STOMAGEN to the ERf/TMM/SERK complexes, which results in autophosphorylation, which in turn leads to sequential phosphorylation of YDA, a protein kinase kinase kinase (MPKKK), MKK4/5/7/9, and MPK3/6, and eventually to the inhibition of SPCH (Bergmann *et al.*, 2004; Lampard *et al.*, 2008; Lampard *et al.*, 2009). This signaling cascade links cell proliferation and cell fate specification to developmental and environmental signals (Lampard *et al*., 2008; Lampard *et al*., 2009).

Clustered stomata occur once one or more pivotal genes such as *YODA* (Bergmann *et al.*, 2004), *ER* and *ERL1* and *ERL2* (Shpak *et al.*, 2005), and *TMM* (Yang & Sack, 1995; Nadeau *et al.*, 2002) mutate. Except genes mentioned above, the dysfunction of *BREAKING OF ASYMMETRY IN THE STOMATAL LINEAGE (BASL)* leads to clustered meristemoids (Dong *et al.*, 2009), and dysfunction of *GLUCAN SYNTHASE-LIKE 8 (CHOR)* leads to clustered stomata (Guesman *et al*., 2010).

<center>Environmental regulation on stomatal lineage formation</center>

In normal development, stomata strictly follow a spacing pattern known as the one-cell spacing rule (Sachs, 1978), which may provide a structural basis for the optimal balance between gas exchange and water loss (Papanatsiou *et al*., 2016). The spacing pattern, however, can be violated if a pivotal gene is mutated, or under abiotic stress. Mutant of abscisic acid deficiency, *aba2-2*, exhibits increased stomata number within a smaller cotyledon, and the increase was prevented by ABA application (Tanaka *et al.*, 2013). Development of stomata is affected by environmental signals such as light, CO_2 and water availability (Qi & Torii, 2018). Clustered stomata are induced under abiotic stress with sugar solution immersion (Atika *et al.*, 2013). In the condition of high salinity, the morphology of stomata can alter to adapt to the high abiotic stress environment (Abbruzzese *et al*., 2009). The stomatal density can be modulated in different ways by several genes for adapting to drought. Dehydrins as a type of protein to response to abiotic stresses, its upregulation is greatly affected by drought treatment, and as the consequence

of overexpression, stomatal density is significantly reduced, thus enhancing drought tolerance (Xie *et al*., 2012).

   Likely involvement of both *ER* and *SUE* in epidermal phenotype in Landsberg *erecta*

In the 1960s, the first *er* mutant was identified from the Landsberg ecotype (Rédei, 1962). This line was thus named Ler and it quickly became a popular plant material for studying reproductive development and many other aspects due to the pleiotropy of *ERECTA*. *ERECTA* is well known for its compact and disk-like inflorescences, as well as the shorten internodes and pedicels. The cloning and molecular analysis of *ER* and *er* showed that it regulates the shape of organs originating from shoot apical meristem, and encodes a putative receptor protein kinase which consists of a cytoplasmic kinase catalytic domain, a transmembrane region, and an extracellular domain of leucine-rich repeats (Torii *et al*., 1996). *ERECTA* is also expressed in the primordia and immature organs (Ryusuke *et al*., 1998). Later ER and its homologs ERL1 and 2 were found to suppress stomatal lineage formation; *erecta* mutations result in the increased stomata density and increased SLGC (Shpak *et al*., 2005).

Our current knowledge about the regulation of stomatal lineage formation is still very limited and additional genes involved in this regulation remain to be identified. It has been found that one or more loci other than *er-1* in Ler enhance the stomatal clustering phenotypes of the *flp* mutants (Lai *et al.*, 2005; Yang, 2016). It was also observed that the abaxial cotyledon epidermis has more epidermal cell numbers Ler than in the Col-0 accession (Yang, 2016). These observations prompted the search for additional gene(s) other than *er-1* that is responsible for the phenotype of increased epidermal cells in Ler. Jenny Swinton in our lab attempted to identify the gene(s) by mapping using DNA polymorphisms between Col-0 and Ler. She collected DNA samples from F_2 plants that were from a cross between Ler and Col-0 and had Ler-like epidermal cell numbers in the cotyledon. This mapping effort led to the identification of small region of interest on chromosome two. In this region, after analysis of DNA polymorphisms between Ler and Col-0, two candidate genes, At2G28990 and At2G29000, both encoding a malectin-like leucine-rich repeat receptor-like kinase, were identified. As one of subfamilies of receptor like kinases with malectin-like domain, *Cr*RLK1Ls are involved in cell growth, reproduction, immunity, and response to environmental stresses (Franck *et al.*, 2018). *THE1* in Arabidopsis, a member of *Cr*RLK1Ls, negatively affect cell wall integrity as its mutant displayed alleviation on hypocotyl growth inhibition by a cellulose synthase deficiency (Haruta *et al*., 2014; Merz *et al*., 2017) and exacerbation on ectopic lignification (Haruta *et al*., 2014). FERONIA*,* another member of *Cr*RLK1Ls in Arabidopsis, also functions in epidermal development as its mutant *fer* produced distorted trichomes (Duan *et al*., 2010), and box-shaped epidermal cells in leaves (Dong *et al*., 2019).

In Ler, At2G28990 is completely deleted, and At2G29000 partially deleted. The *at2g29000* sequence in Ler lost most of the coding region spanning from the start codon to part of the second last exon that would normally encode the kinase domain of the LRR-RK (**Fig. 3. C;** Blum *et al.*, 2020). Alignments in NCBI Blast indicate that the At2G28970 protein is the closest homolog of At2G28990 with 74% identities, and At2G28960 is the closest homolog of At2G29000 with 60.2% identities. Both At2G28960 and At2G28970 are not affected in Ler comparing to their protein sequences in Col-0. Considering the higher homology between At2G28990 and At2G28970 than between At2G29000 and At2G28960, it is hypothesized that the loss of At2G28990 likely has a smaller impact on stomatal lineage formation than the loss of At2G29000, if both are involved in the regulation. Therefore, my thesis research focused on At2G29000.
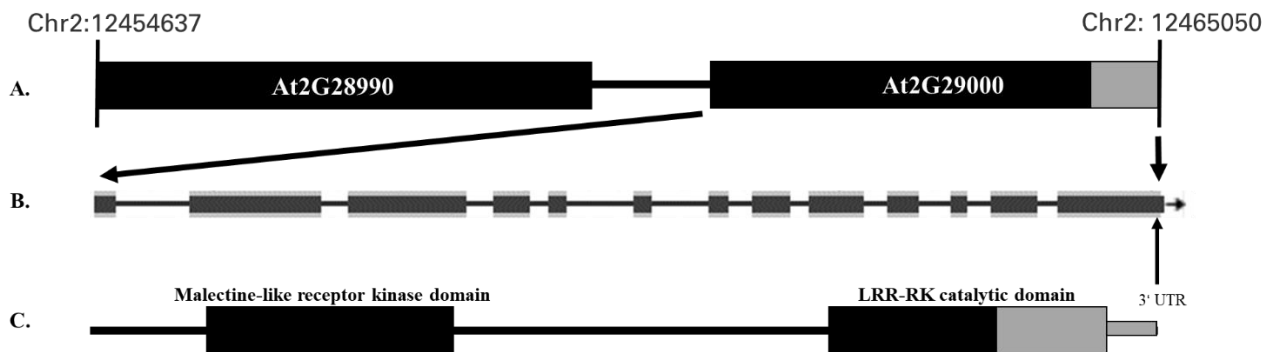

Fig. 3. A) Positions of At2G28990 and At2G29000 on chromosome 2 in Col. B) Structure of At2G29000 in Col. C) The N-terminal Malectin and the C-terminal kinase domains in At2G29000. In **B,** black boxes with grey margins: exons; lines between exons: introns; In **A** and **C**, grey regions represent the remaining sequences of At2G29000 in Ler.

I hypothesize that the double mutations of *er-1* and *at2g29000* (Ler) result in the epidermal phenotype in the cotyledon in Ler. Indeed, I found the epidermal cell numbers in the *er-1* single mutant were significantly higher than those in Ler which the *at2g29000* mutation was rid of through genetic segregation. This observation indicates that *at2g29000* partially suppressed the epidermal phenotype of *er-1* in Ler. We thus named the At2G29000 locus *SUPPRESSOR OF ERECTA* (*SUE*) and its mutant allele in Ler *sue-1*. Building on this finding, I went on to characterize the epidermal phenotypes in a second set of single and double mutants, including a T-DNA insertion mutant of *SUE*, *sue-2*, and a T-DNA insertion mutant of ER, *er-124*, as well as their double mutant, and in plants with heterozygosity at one or two of these loci for the two sets of mutant alleles. Decreased trichome numbers were also observed in all the *er* and *sue* mutants studied. The results also suggest that At2G28980 may play a role similar to that of At2G29000. This research uncovered a novel class of LRR-RKs in regulation of epidermal cell production and they may interact with ER at the same node of a genetic network.

CHAPTER II

PLANT MATERIAL AND METHODS

Plants and Growth Conditions

Murashige and Skoog (MS) agar medium was used for plate planting for epidermal phenotyping in cotyledons. MS medium consists of 4.3g/L GIBCO™ Murashige and Skoog salt base, 10g/L sucrose and 7g/L agar.

Sunshine MVP growing Mix was used for soil planting. For counting trichomes, genotyping by PCR, examining inflorescence morphology for identifying *er* mutant plants, seeds were either directly planted on soil or seedlings were transplanted to soil 2-3 weeks after seed germination on the agar medium.

Plants were grown in a growth chamber at 22°C, with an illumination regime of 14-hour light/10-hour darkness and 50 umol/m^{2}s light intensity.

Data Collection and Statistical Analyses

Photos of cotyledons were taken using a Nikon SMZ1000 dissecting microscope with a combination of 0.5X and 3X lenses and a Nikon DS-Ri1 digital camera and NIS-Elements BR 4.40.00 software. Cotyledon areas were measured with SigmaScan Pro5.

Cotyledons were collected from every line of mutants, and epidermal cells were counted in randomly selected seven fields in each cotyledon under a 100X objective lens on a Nikon Eclipse 80i compound microscope. Cell densities were determined based on the cell numbers in the seven microscopic fields and the total cell numbers were calculated by multiplying the cell densities with the corresponding cotyledon areas. The numbers of cotyledons used for the data collection are listed in **Table 1**.

Trichomes on the first pair of leaves were counted when plants were at least two weeks old under the Nikon SMZ1000 dissecting microscope. Seeds were planted on Sunshine MVP growing Mix soil. First pair of leaves were collected from 10 seedlings for each genotype.

One-way ANOVA (P<0.05, Game-Howell test) analysis was conducted in IBM SPSS Statistics 26 for examining significance level. Student's *t*-test (P<0.05) was also conducted in Excel for part of the data. Histograms were drawn in GraphPad Prism 8.

	Genotype	Adaxial	Abaxial
Set1	*ERER SUESUE* (Col)	20	20
	sue-1	30	60
	er-1	20	40
	ER/er-1 sue-1/sue-1	5	13
	er-1/er-1 SUE/sue-1	6	7
	ER/er-1 SUE/sue-1	10	10
	er-1 sue-1 (Ler)	10	20
Set2	*sue-2*	10	20
	er-124	10	20
	er-124 sue-2	10	20
	ER/er-124 SUE/sue-2	10	10

Table. 1. Sample size of cotyledons for all mutants characterized.

GUS Staining

Composition of GUS staining solution: 50mM sodium phosphate buffer, pH=7, 1mM EDTA, 0.1% Triton X-100, 100ug/ml Chloramphenicol, 1mg/ml X-Gluc, 2mM Ferricyanide, 2mM Ferrocyanide. 10 promoter GUS lines (*SUE:GUS*) and 9 protein GUS lines (*SUE:SUE-GUS*) were examined and characterized. Representative lines of *SUE:GUS 2-1* and *SUE:SUE-GUS 2-3* were photographed.

For GUS staining, fresh plant materials were collected and immersed in the GUS staining solution. The samples were incubated in the dark at 37 °C for 48 hours. Then the GUS staining solution was replaced with 70% ethanol for multiple times at room temperature until the plant tissue was completely white.

Light Microscopy

Fresh or fixed (in 70% ethanol) plant materials were wet-mounted and observed on a Nikon Eclipse 80i compound microscope under the bright field with or without the differential interference contrast (DIC) optics. Photos were captured using a Nikon digital sight DS-Ri1 camera and the NIS-Elements BR 4.40.00 software.

DNA Extraction

To extract DNA, fresh Arabidopsis inflorescences or leaves were ground in a 1.5ml microcentrifuge tube in 300ul 2x cetyl-trimethyl-ammonium bromide (CTAB) buffer and incubated at 65 °C in a water bath for at least 10mins (up to hours). After the incubation and cooling, 300ul chloroform were added and vortexed thoroughly. The samples were then spun in a microfuge at 13200 rpm (rounds per minute) for 5 minutes to separate the chloroform from the aqueous phase. The upper aqueous portion was transferred to a new microcentrifuge tube, and 300ul 2-propanol were added and vortexed. The sample was then spun in a microfuge at 13200 rpm for 5min to pellet the DNA. The supernatant was removed, and the DNA pellet was washed with 500ul 70% ethanol. After a brief spin in a microfuge, the 70% ethanol was carefully removed, and the DNA pellet was air dried. The DNA sample was re-suspended in TE buffer (10 mM Tris, pH 8.0; 1 mM EDTA, pH 8.0) or DD H_2O.

Polymerase Chain Reactions (PCR)

PCR program: 95°C 3 minutes; 95°C 1 minute; 62°C 1 minute; 72°C 1.5 minutes (35 cycles); 72°C 5 minutes. PCR was carried out in a BIO-RAD T100 Thermal Cycler.

PCR sample mix: QIAGEN Tap PCR Master Mix, 10uL; QIAGEN RNase Free water, 7uL; Forward and reverse primers, 1uL; DNA sample, 1uL. Final volume was 20uL.

PCR Product Purification and Sequencing

PCR products were purified using a QIAquick PCR purification Kit according to the manufacturer's procedure, except that the DNA sample was eluted in 20uL water.

Purified PCR product was submitted to the DNA/Protein Core Facility of Oklahoma State University for sequencing. Sequence files were analyzed in FinchTV 1.4.0.

Seeds Sterilization

Seeds were poured into a 1.5mL tube and 1mL ethanol was added into the tube. The tube was then inverted several times for mixing and was let to stand for 10 minutes. The ethanol was carefully poured off and 1mL bleach solution (20%-30%) was added. The tube was inverted several times again for mixing and then let stand for 10 minutes. The bleach solution was replaced with 1mL sterile DD H_2O for washing the seeds for 10 minutes. The seeds were washed three washes before planted on the agar medium.

Gel Electrophoresis and Imaging

Gels used for electrophoresis is 1% agarose gel in the Tris-acetate-EDTA (TAE) solution and PHENIX RESEARCH GelRed 10,000X in Water were added to the gel for visualizing the PCR products. Fisher Biotech Electrophoresis System FB400 and BIO-RAD MINI-SUB CELL GT were used for agarose gel electrophoresis. Gels were examined and photographed using proteinsimple AlphaImager HP with AlphaImagere HP 3.4.0.

CHAPTER III

RESULTS

SUE is expressed in stoma-containing cell clusters in the cotyledon and additional cell types in other organs

The hypothesized function of *SUE* likely requires its expression in epidermal cells. To determine its expression pattern, transgenic Arabidopsis lines containing a β-glucuronidase (GUS) reporter gene fused with either a *SUE* promoter (*SUE:GUS*) or *SUE* promoter plus its coding region (*SUE:SUE-GUS*) were generated (by Yixing Wang in our lab). I characterized the *GUS* expression patterns in these lines. The different lines exhibited similar GUS-staining patterns although the intensities of the GUS signal varied. The GUS signals were primarily found in the distal tip of cotyledon on 5-day old seedlings and some stomata (**Fig. 4A**). In 5-11-day older seedlings, the GUS signal were in a large portion of, but not all, stomata and their surrounding epidermal cells (**Fig. 4C-D**). The GUS signals on the adaxial side of the cotyledon appeared to be stronger than on the abaxial side (**Fig. 4E**). GUS signals were also found in young leaf tip, vascular bundles, a subset of trichomes and root hairs (**Fig. 4C**). GUS signals in the *SUE:SUE-GUS* lines were weaker than the signals in the *SUE:GUS* lines (**Fig. 4A, B, and D**). In the cotyledon, mesophyll beneath the GUS-positive adaxial stomata contained strong GUS signals, which were clearly seen from the abaxial epidermis. These results suggest that *SUE* is expressed in a portion of cell clusters with each cluster containing a stoma and its neighboring cells in both the epidermis and the mesophyll and at a higher level on the adaxial side than on the abaxial side in the cotyledon. *SUE* is also expressed in portions of trichomes and root hairs and in the vascular tissue.
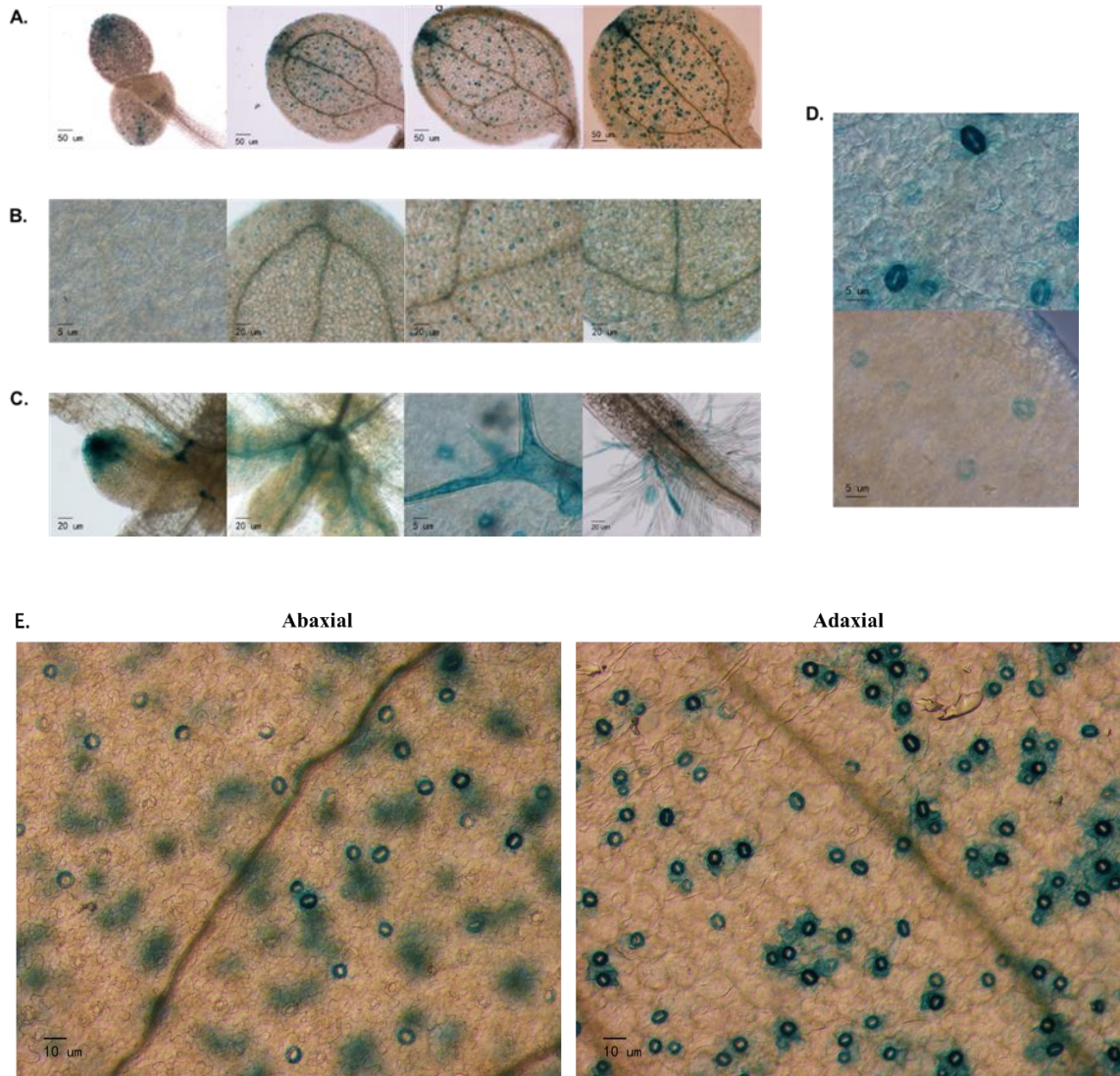
Fig. 4. GUS expression patterns. A, C and E *SUE:GUS*; **B** *SUE:SUE-GUS*. **A** and **B**, Cotyledons of abaxial from 5-day, 7-day, 9-day, and 11-day old seedlings (from left to right), respectively. **C**, images showing GUS signals in a young leaf, vascular bundles of leaves, a trichome, and some root hairs (from left to right) of a 12-day old seedling, respectively. **D**, close-up views of GUS signals in stomata and surrounding cells in abaxial cotyledon of the *SUE:GUS* line in **A** (upper panel) and weaker GUS signals in the *SUE:SUE-GUS* line in **B** (lower panel,). **E** GUS signals seen on the abaxial and adaxial epidermis of the same cotyledon from a 11-day old seedling of the line in **A**.

13

Isolation of mutants of various allele combinations at the *ER* and *SUE* loci

To investigate the genetic interactions between *er* and *sue* mutations, mutant lines containing a variety of allele combinations at the *ER* and *SUE* loci were isolated. These lines included two sets of single and double mutants and lines harboring a homozygous mutation at one locus and heterozygous mutation at the other locus or heterozygous mutations at the two loci. Set1 of single and double mutants and its wild-type control consisted of *er-1*, *sue-1*, Ler (double mutant of *er-1 sue-1*), and Col-0. To isolate the *sue-1* and *er-1* mutants, F₃ lines likely homozygous at one of the two loci and heterozygous at the other locus according to earlier mapping data were chosen. The *sue-1* mutation was identified by specified PCR products. One PCR product could be amplified the *sue-1* allele while the other only from the *SUE* allele. The presence or absence of the *er-1* allele was confirmed by the presence or absence of the phenotype of compact inflorescence, short pedicle, and short inflorescence stem (Torii *et al.*, 1996) in one (when *er-1* was homozygous) or two generations (when *er-1* was heterozygous), and by DNA sequencing for detecting the point mutation in *er-1* (**Fig. 6A**). As shown in **Fig. 5A**, three single *sue-1* plants and two single *er-1* plants were successfully isolated. They were used for later epidermal cell studies. The F₃ lines for identifying these single mutants were also used to identify the mutant lines that harbor a homozygous mutation at one locus and a heterozygous mutation at the other locus. The genotypes were *ER/er-1 sue-1sue-1* and *er-1er-1 SUE/sue-1*. Genotypes at the *SUE* locus were determined by PCR (**Fig. 5C**, **Fig. 5D**) and genotypes at the *ER* locus were determined by sequencing a PCR product amplified from the *er-1* mutation region or inflorescence phenotypes in the next generation (**Fig. 6**). Epidermal cell data were collected before the verification of the genotypes. After collecting the data, plants were transplanted to soil for later genotyping. 18 *ER/er-1 sue-1/sue-1* and 13 *er-1/er-1 SUE/sue-1* heterozygous mutants were successfully isolated. Only the data from the correct genotypes were included in the analyses. In addition, crosses between Col-0 and Ler were performed (Ming Yang) to obtain the *ER/er-1 SUE/sue-1* F₁ plants.

The Set1 single and double mutants involved two very different genetic backgrounds of Col-0 and Ler, which may complicate the investigation. To provide additional evidence on the interaction between an *er* mutation and a *sue* mutation in the same genetic background, another set of single and double mutants were employed. Set2 of the single mutants included *er-124* (SALK_044110) and *sue-2* (SALK_012698) that were T-DNA insertion mutants in Col-0 previously confirmed by Yixing Wang in the lab. Crosses between *er-124* and *sue-2* were performed (Ming Yang). DNA samples were collected from 91 of the F₂ plants for PCR genotyping at the *SUE* locus, which resulted in the identification of seven *sue-2* heterozygous plants. Three of the seven lines were confirmed to be *er-124* homozygous based on inflorescence phenotype (**Fig. 6C**) and *sue-2* homozygous in the F₃ generation (**Fig. 5B**). The F₁ plants were used as the double heterozygote of *er-124* and the *sue-2*.

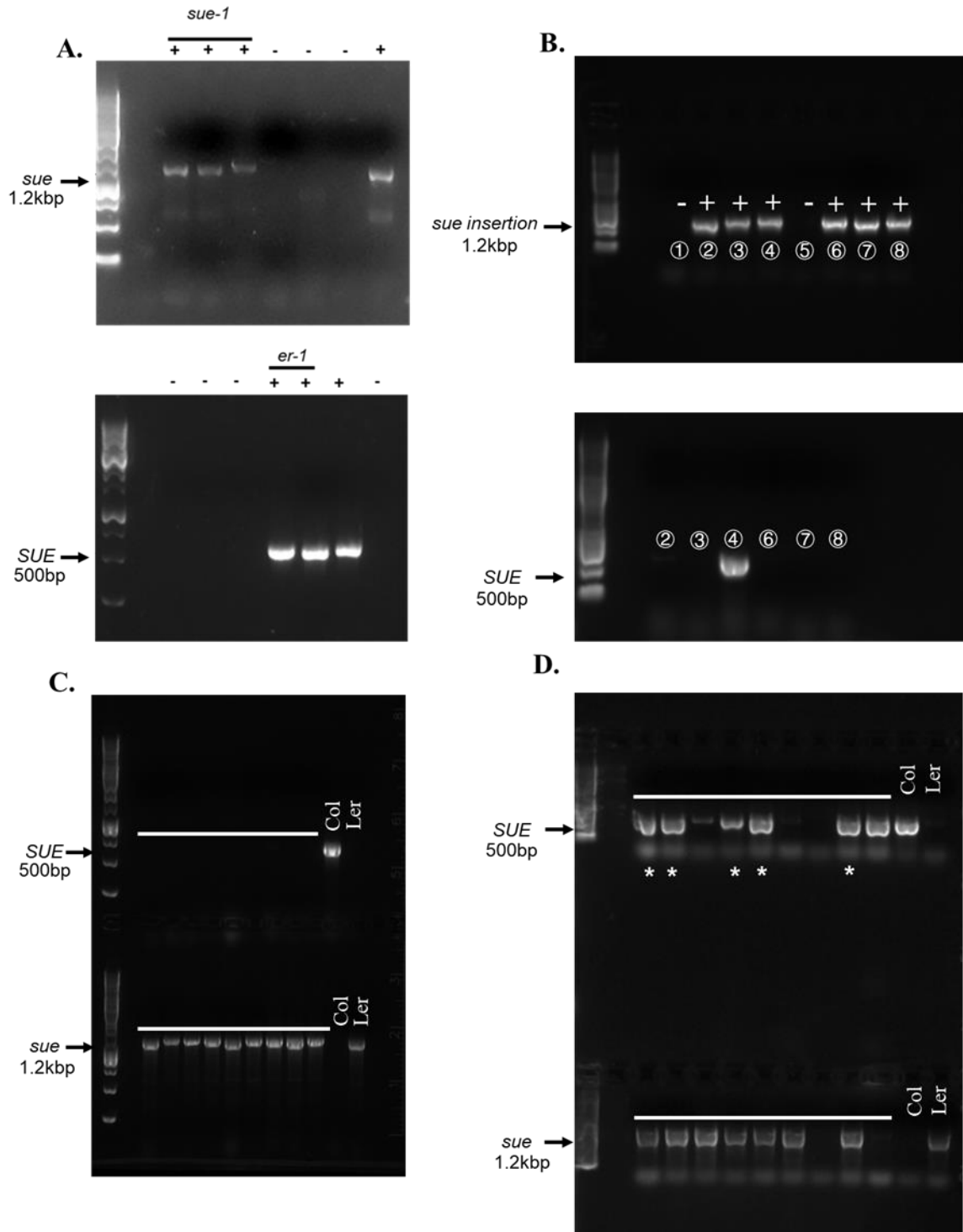**Fig. 5. Genotyping at the *SUE* locus using PCR. A.** Electrophoresis result of PCR products for screening *sue-1* for Set1. *sue* and *SUE* are amplified by different pairs of primers. First five samples are F4 progeny from the cross of Col-0 and Ler. Last two samples are Col-0 and Ler for severing as positive and negative controls, respectively. + and – indicate amplified and non-amplified PCR results, respectively.

B. Electrophoresis result of PCR products for screening *er-124 sue-2* for Set2. Mutants with only *sue* insertion are desired mutants, which are ②, ③, ⑥, ⑦, ⑧. Five mutants were then screened again based on phenotypes for *er* mutation. + and – indicate amplified and non-amplified PCR products, respectively.

C, **D**. Electrophoresis results of PCR products for isolating heterozygous mutants from the cross of Col and Ler. The left panel is for the isolation of *sue-1/sue-1 ER/er-1* mutants (**C**) and right is for *er-1/er-1 SUE/sue-1* mutant (**D**). All plants in **C** are *sue-1* homozygous, plants in **D** which are indicated by * are *sue-1* heterozygous mutants.
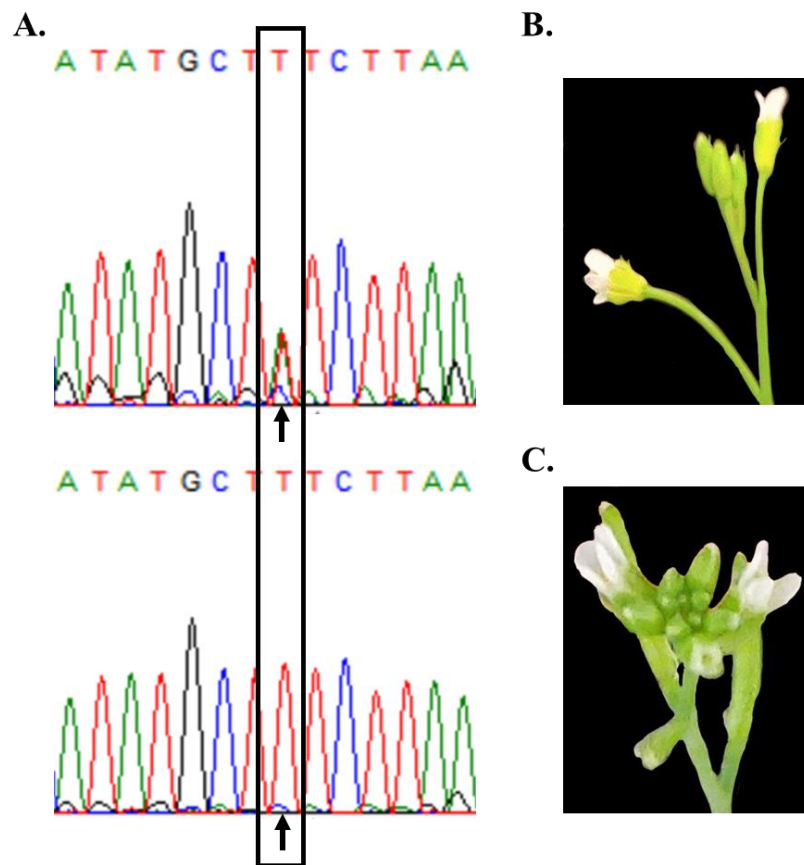
Fig. 6. Sequences of *er-1* and inflorescences phenotypes. A. Sequences of *er-1* PCR product. The arrow points at the point mutation of *er-1* in Ler. This base is mutated from A (Col-0) to T (Ler) in the *er-1* mutation. Upper panel shows the double peaks of A and T bases in a heterozygous *er-1* plant; Lower panel shows the homozygous mutation of *er-1* with T base solely. **B.** Typical Col-0 inflorescence phenotype with dispersed floral buds and flowers. Heterozygous *er-1* or heterozygous *er-124* plants exhibited similar inflorescence morphology. **C.** Typical *er-124* homozygous inflorescence phenotype with

compact floral buds and flowers. The *er-1* homozygous mutant exhibited similar inflorescence morphology, which flower buds are.

Characteristics of epidermal cells in the cotyledons in Set1of single and double mutants

Since *SUE* is expressed in some stoma-containing cell clusters in both the adaxial and abaxial epidermis of the cotyledon, I first investigated epidermal cell numbers in 14-day old cotyledons in Set1 of the single and double mutants and the wild-type Col-0. Three *sue-1* lines and two *er-1* lines isolated from the F$_4$ plants were used in this investigation.

The *er-1* mutant had significantly more pavement cells, guard cells, meristemoids, and total cells in the adaxial epidermis than Col-0 and Ler (**Fig. 8A;** ANOVA, P < 0.05). The cell numbers in *er-1* were approximately 1.9 to 2.8 folds of those in Col-0, and they, excluding the meristemoid number, were approximately 1.5, 1.9, and 1.7 times of those in Ler, respectively (**Table 2**). These differences, except that of the meristemoids, were significant between *er-1* and Ler (ANOVA, P < 0.05). On the other hand, *sue-1* had significantly fewer guard cells and total cells than Col-0 (ANOVA, P < 0.05), with 30% and 20% decreases in these two cell types, respectively. The *sue-1* mutant and Col-0 did not differ in the numbers of pavement cells and meristemoids (ANOVA, P > 0.05). The results on the abaxial epidermis were similar to those on the adaxial epidermis, except that the number of meristemoids was significantly larger in *sue-1* than in Col-0 and the numbers of total cells were not significantly different between the two genotypes (**Fig. 8A**; **Table 2**). These results indicate that *sue-1* had a mild negative effect on cell production in the adaxial epidermis and partially suppressed the positive effect of *er-1* on epidermal cell proliferation in Ler.

Because *sue-1* plays a negative role in epidermal cell proliferation and the mapping of *sue-1* was based on a Ler-like (increased epidermal cells) phenotype (**Fig. 8A**) and the DNA polymorphisms in Ler, I hypothesized that heterozygous *sue-1* should promote epidermal cell production when *er-1* is homozygous or heterozygous. To test this hypothesis, epidermal cell numbers in *ER/er-1 sue-1sue-1*, *er-1er-1 SUE/sue-1*, and *ER/er-1 SUE/sue-1* were determined. Indeed, the numbers of the three cell types and the total cells in *er-1er-1 SUE/sue-1*, and *ER/er-1 SUE/sue-1* were either similar to or more than those in Ler in both the adaxial and abaxial epidermis (**Fig. 8B**). The *ER/er-1 sue-1sue-1* plants were similar to the single *sue-1* homozygous mutant in terms of having a mild negative effect on the epidermal cell production (**Fig. 8**). These results demonstrate that it is possible that the mapping was actually partially based on the combined effect of heterozygous *sue-1* and an *er-1* mutation on epidermal cell production. When checking the mapping data, it was found that heterozygous or homozygous Ler markers near the *SUE1* locus were always concurrent with heterozygous or homozygous Ler markers, but not with Col-0 homozygous markers, near the *ER* locus. These findings support the above hypothesis.

17

The ANOVA analysis did not detect a difference in the total epidermal cell number in the adaxial epidermis and in the guard cell number in both the adaxial and abaxial epidermises between Col-0 and Ler. However, the multiple-genotype comparisons in ANOVA might not be sensitive enough for detecting subtle differences between Col-0 and Ler. Therefore, pairwise comparisons between Col-0 and Ler were carried out with *t*-test to detect possible subtle differences. These comparisons confirmed the differences between Col-0 and Ler already detected in the ANOVA analysis and revealed that Ler also had more total epidermal cells in the adaxial epidermis than Col-0 ($P < 0.05$) although their guard cell numbers were not statistically different ($P > 0.05$; **Fig. 9**)

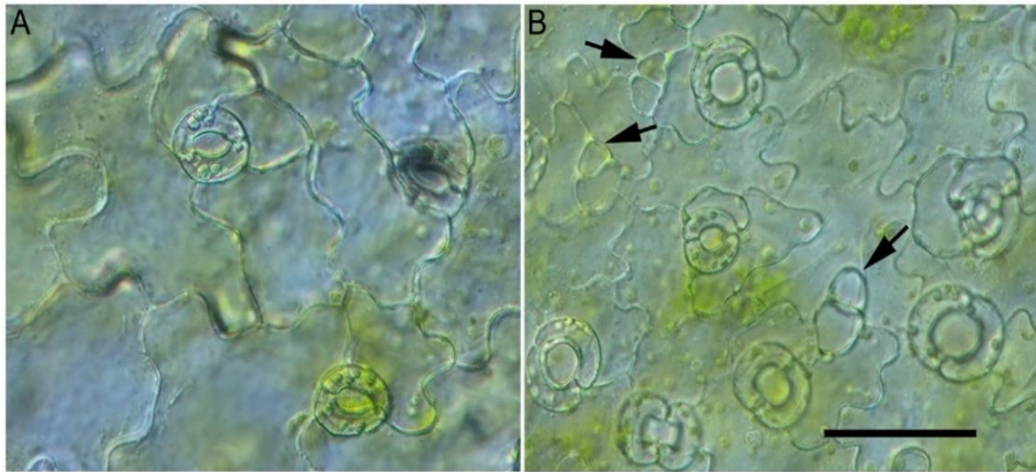**Fig. 7. Abaxial epidermal phenotypes in mature cotyledons.** (A) Col-0. (B) Ler-0. Cotyledons were from seedlings of $\geq$ 14-day old at the time of photographing. Arrows indicate meristemoids. Scale bar $= 20$ μm for both images.
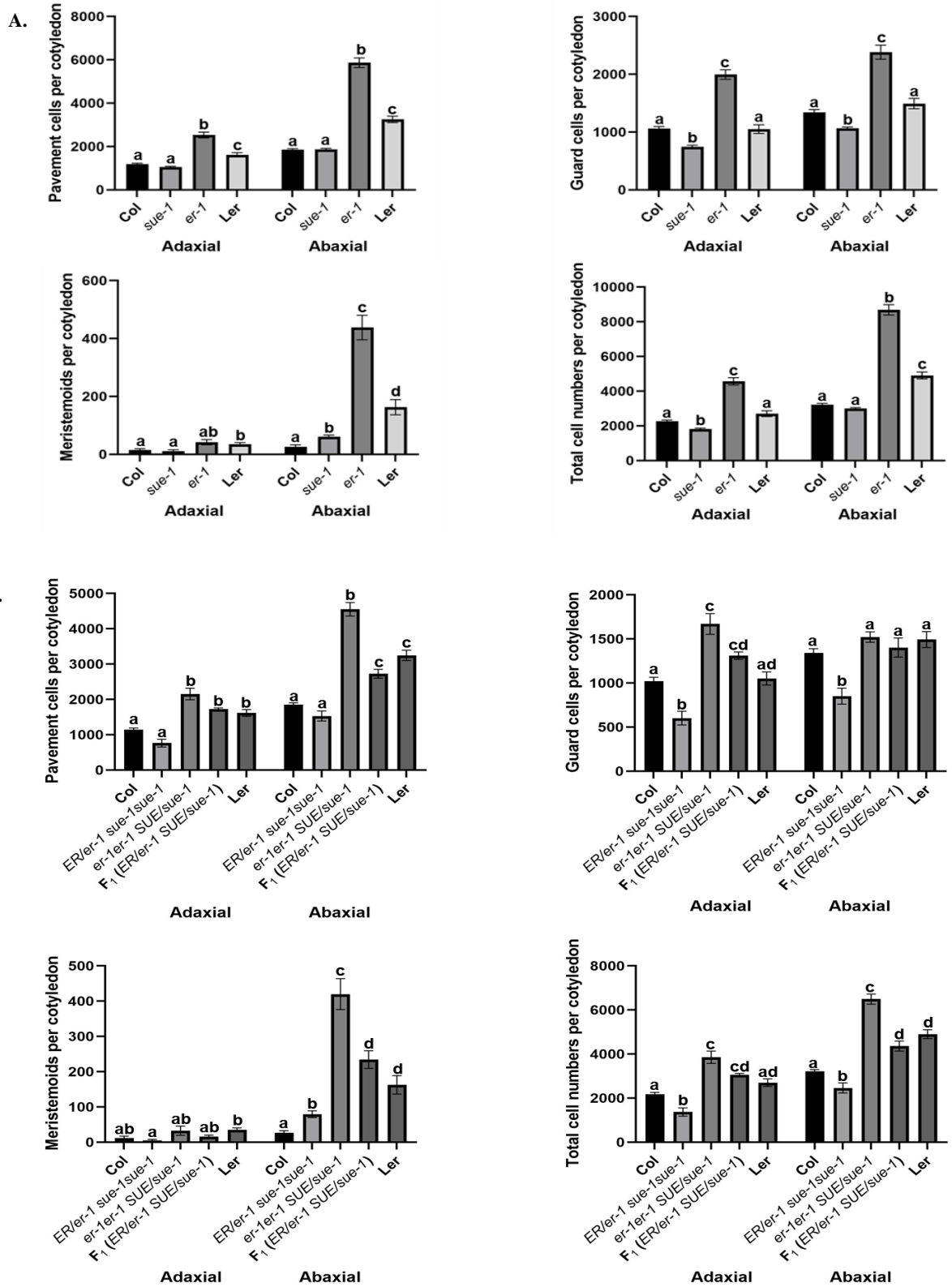
Fig. 8. Epidermal cell characterization of Set1 mutants on adaxial side and abaxial side of cotyledon. **A.** Homozygous mutants of Set1; **B.** Heterozygous mutants of Set1.

Shown are means ± standard errors. Different letters above bars indicate significant differences level (P < 0.05).
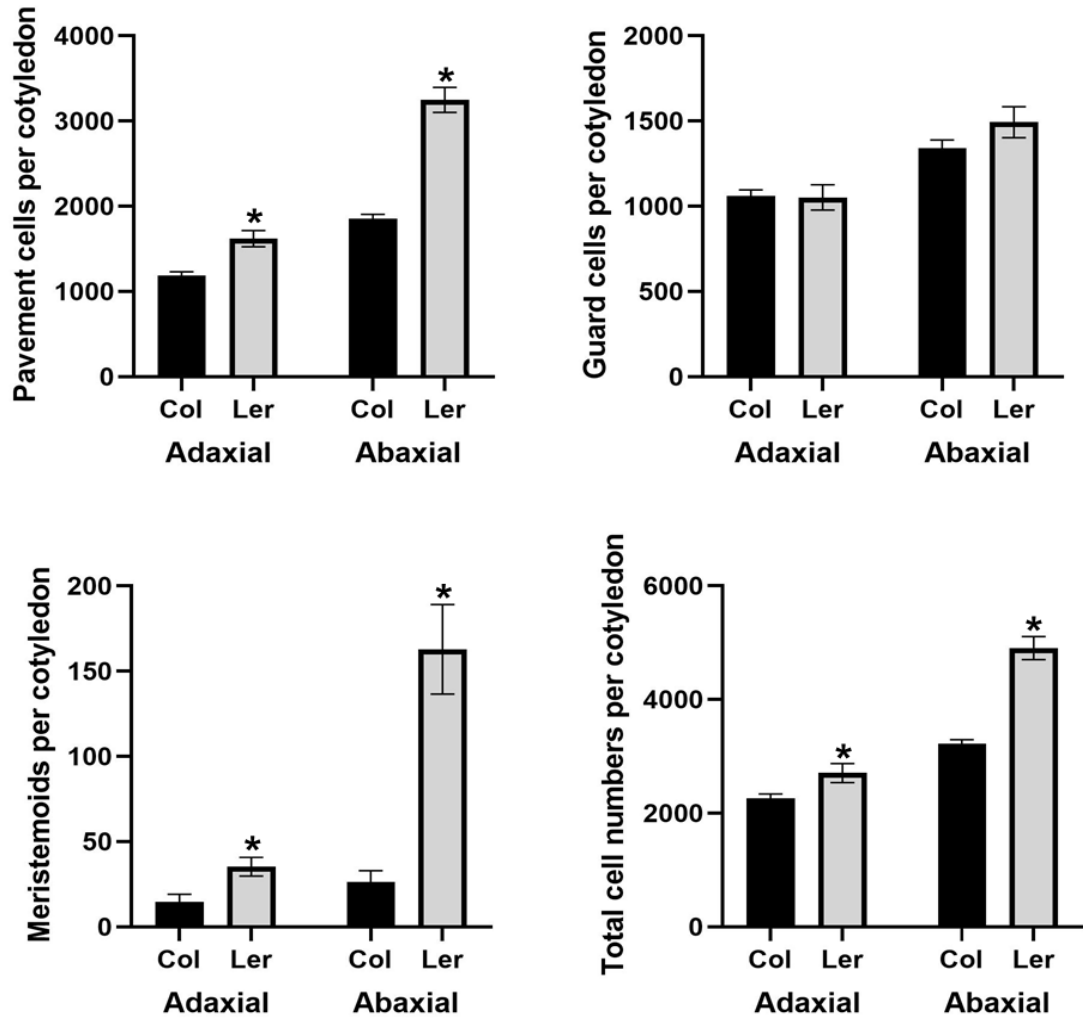
Fig. 9. Epidermal characterization of Col and Ler. * indicates significant difference (*t*-test, P<0.05). Shown are means ± standard errors.

Characteristics of epidermal cells in the cotyledons in Set2 of single and double mutants

Quantifying the epidermal cell numbers in the single and double mutants of Set2 should provide additional evidence on the function of SUE and its genetic interaction with ER in epidermal cell production. Similar to *sue-1*, *sue-2* had reduced guard cells and the total epidermal cells in the adaxial epidermis in the cotyledon comparing to Col-0 (**Fig. 10A; ANOVA, P < 0.05**). The reductions were small, i.e., 5% and 10%, respectively (**Table 2**). Unlike *sue-1*, *sue-2* did not differ from Col-0 in any of the cell numbers in the abaxial

epidermis (**Fig. 10A**; ANOVA, P > 0.05). The *sue-2* mutation also suppressed the positive effect of *er-124* in the abaxial epidermis as the pavement cells and the total epidermal cells in the *er-124 sue-2* double mutant showed significant reductions of 33% and 20%, respectively, when compared with the *er-124* single mutant (**Fig. 10A**; ANOVA, P < 0.05). However, no such suppression by *sue-2* was observed to any of the cell types and the total epidermal cells in the abaxial epidermis in *er-124 sue-2* (**Fig. 10A**; ANOVA, P > 0.05). Moreover, *ER/er-124 SUE/sue-2* did not differ from Col-0 on any of the cell types and the total epidermal cells (**Fig. 10B;** ANOVA, P > 0.05), except that its abaxial meristemoids were nearly five times more than that in Col-0 (**Fig. 10B**; ANOVA, P < 0.05; **Table 2**). These findings are in agreement with the findings on the function of SUE and its relationship with ER in the Set1 investigation, although they also suggest that *sue-2* is weaker than *sue-1* in suppressing epidermal cell production.

Fig. 10. Epidermal cell characterization of Set2 mutants on adaxial side and abaxial side of cotyledon. **A.** Homozygous mutants of Set2; **B.** Heterozygous mutants of Set2. Shown are means ± standard errors. Different letters above the bars indicate statistically significant differences ($P < 0.05$).
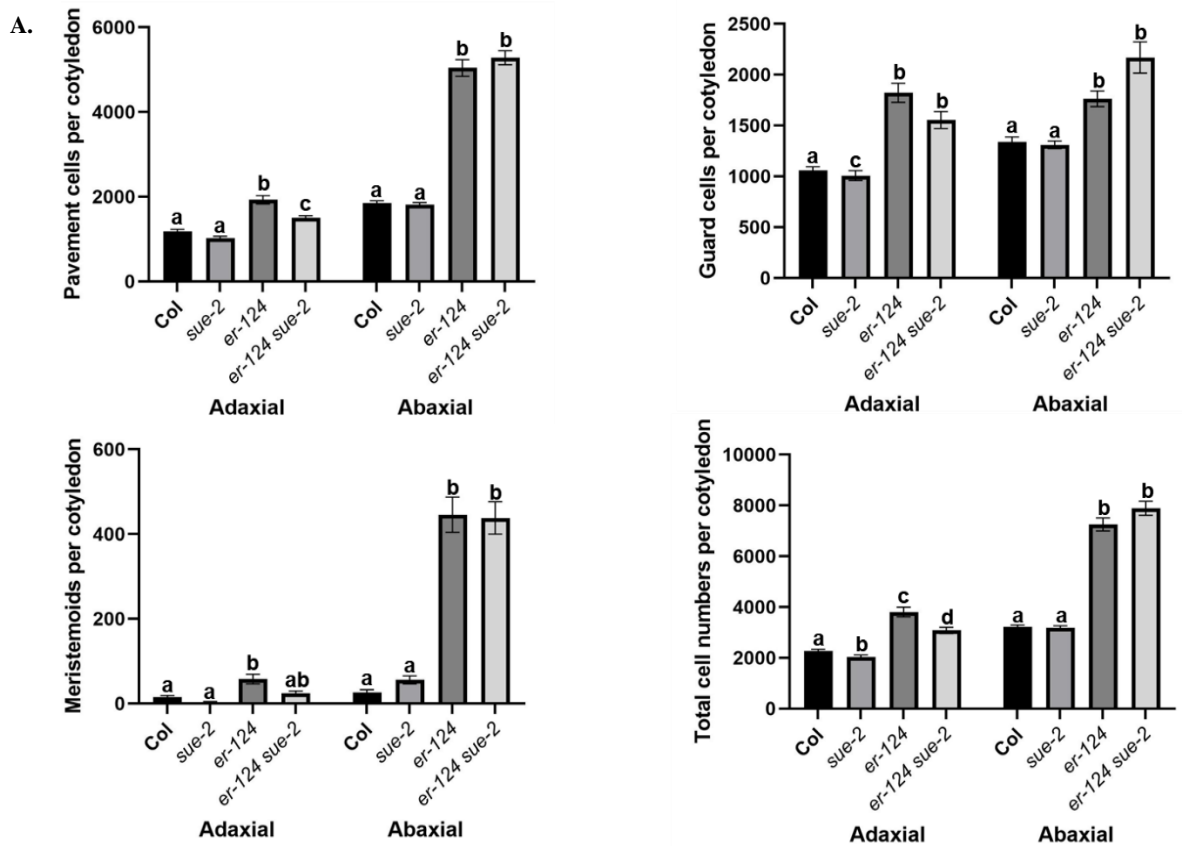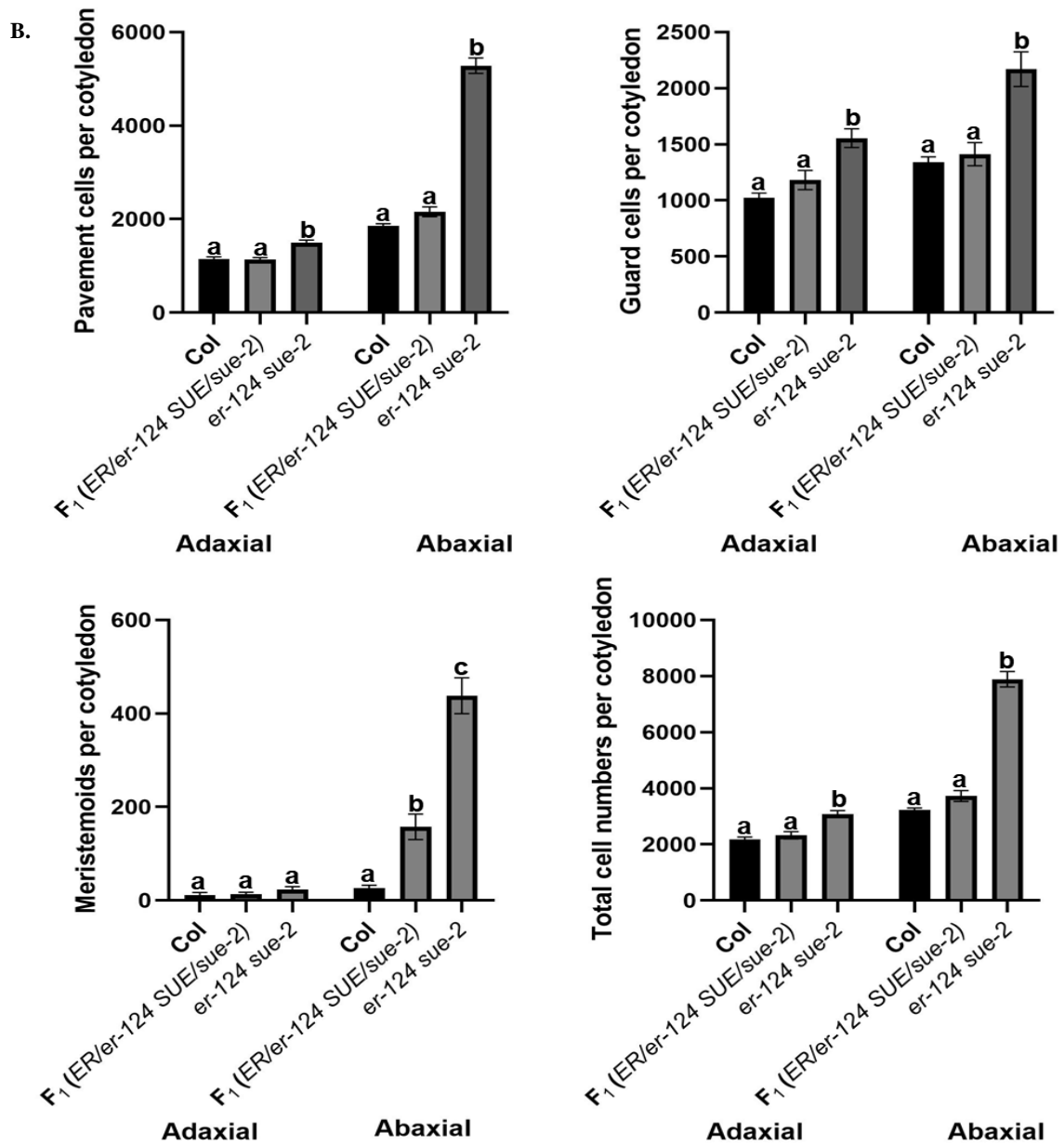
	Pavement cells	Guard cells	Meristemoids	Total cells
Col	1.000	1.000	1.000	1.000
	1.000	1.000	1.000	1.000
er-1	2.134	1.884	2.838	2.021
	3.164	1.777	16.536	2.697
sue-1	0.889	0.703	0.767	0.801
	1.009	0.794	2.302	0.930
ER/er-1 sue-1/sue-1	0.645	0.568	0.325	0.607
	0.826	0.635	2.996	0.765
er-1/er-1 SUE/sue-1	1.818	1.577	2.205	1.707
	2.451	1.129	15.947	2.012
F$_1$ (ER/er-1 SUE/sue-1)	1.461	1.237	1.051	1.353
	1.471	1.046	8.847	1.355
Ler	1.367	0.992	2.379	1.198
	1.751	1.114	6.147	1.522
er-124	1.626	1.719	3.894	1.685
	2.719	1.315	16.831	2.251
sue-2	0.860	0.951	0.200	0.898
	0.977	0.979	2.110	0.987
F$_1$ (ER/er-124 SUE/sue-2)	0.955	1.116	0.893	1.030
	1.163	1.054	5.944	1.157
er-124 sue-2	1.265	1.468	1.611	1.363
	2.848	1.619	16.534	2.449

Table. 2. Ratios of mutant cell numbers to those of Col. The upper and lower rows of each genotype are adaxial and abaxial ratios, respectively.

Trichome numbers are reduced in the *er* and *sue* single and double mutants

Because *SUE* is also expressed in the trichomes according to the *SUE:GUS* study, I investigated whether trichome numbers are affected in the single and double mutants of Set1 and 2. I found that Col-0 had an average of 40 trichomes per leaf, the highest among all the genotypes studied (**Fig. 11**). Compared to Col-0, the trichome numbers were reduced approximately by half in *sue-1* and *er-1*, and by even more in Ler ((**Fig. 11**; ANOVA, $P < 0.05$). These results indicate that *er-1* and *sue-1* together had a greater effect on the trichome number reduction than the mutants alone. Consistent with the results of the epidermal cells in the cotyledon, *sue-2* was weaker than *sue-1* in reducing the trichome number and it did not cause a further reduction of the trichome number in *er-124 sue-2*

when compared with *er-124* (**Fig. 11**). These results demonstrate that both SUE and ER play a positive role in trichome production in the wild type.
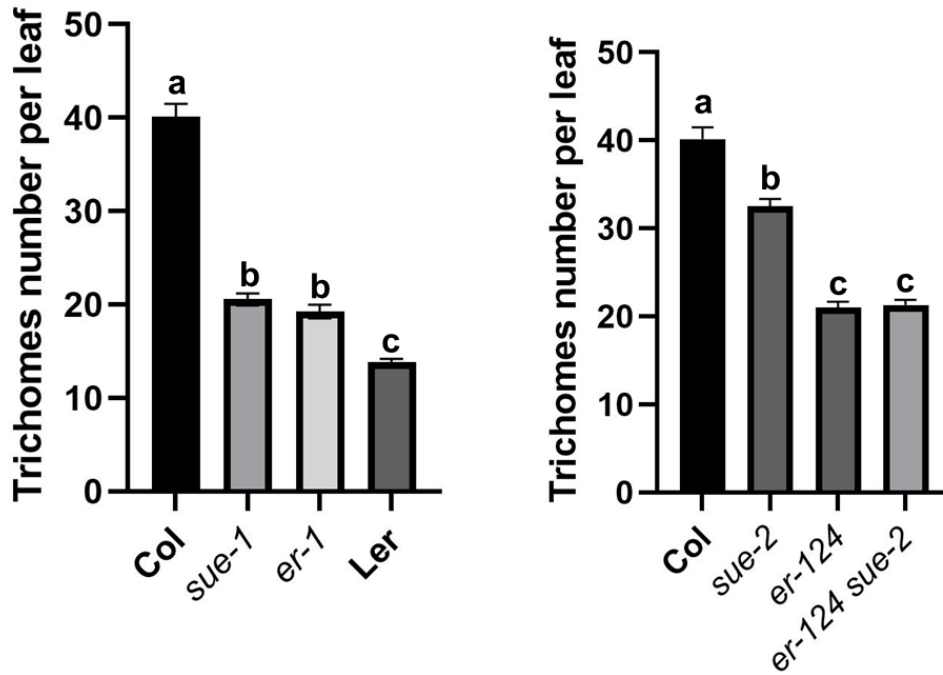

Fig. 11. Numbers of trichomes per leaf in Set1 and 2 single and double mutants. Shown are means ± standard errors (n=20). Different letters above the bars indicate statistically significant differences (P < 0.05).

The likely involvement of At2G28990

The earlier results show that the effect of *sue-2* on epidermal cell production was weaker than *sue-1*. This phenomenon may result from either *sue-2* being a weaker allele compared to *sue-1* or *sue-1* containing an additional mutation or mutations inherited from Ler. As described earlier (page 7), the same deletion caused the loss of both At2G28990 and *SUE* in Ler. Therefore, the more severe effect of *sue-1* may actually result from two loss-of-function mutations at the At2G28990 and *SUE* loci (**Fig. 3**). To investigate this possibility, I determined the genotypes at the At2G28990 locus in the F_3 population from which the *sue-1* single mutant was isolated. Seven *er-1er-1 SUE/sue-1* plants were identified as heterozygous for the *at2g28990* mutation. In addition, homozygous wild-type At2G28990 was found to be linked with homozygous wild-type *SUE* in an *er-1* plant, and homozygous mutant *at2g28990* to be linked with homozygous *sue-1* in two *sue-1* plants. Therefore, *sue-1* used in this investigation was very likely to be an *at2g28990 sue-1* double mutant, raising the possibility that the reported effect of *sue-1* is actually that of this double mutant. The

linkage between the two mutations is certainly expected, given that they are neighboring genes. The current evidence for the role of At2G28990 in the regulation of epidermal cell production is preliminary, but it is not difficult to envision that both At2G28990 and SUE participate in the same pathway because they are homologs.

CHAPTER IV

DISCUSSION

The significance of quantifying epidermal cells to understand gene functions

Landsberg *erecta*, as a well-known material in Arabidopsis, has been studied for years and its unique phenotype is often attributed to the *erecta* mutation. Research on *erecta* phenotypes focused on the morphology of inflorescence, pedicel length, plant height, and cellular phenotypes in certain areas of the epidermis of an organ. In fact, most of the studies of epidermal development in plant mutants focused on cellular phenotypes in certain areas of the epidermis of an organ without addressing how these mutants affect the total numbers of cells in the epidermis. To explore the function of *SUE* and *ER* in epidermal development, I conducted an investigation focusing on the total numbers of cells in the adaxial and abaxial epidermises in the cotyledon. The total numbers of all three cell types, including pavement cells, guard cells, meristemoids, and their sum were determined. This investigation revealed effects of mutations that would have unlikely been found if the total numbers of cells were not determined. As shown **in Fig. 8 and Fig. 10**, the *er* single mutants significantly outnumbered Ler in the numbers of epidermal cells. This hyper-production of epidermal cells caused by the *er* mutations has not been reported before and requires an explanation that the *sue* mutations at least partially provided. This investigation demonstrates that determining the total cell numbers enabled the discovery of the role of SUE and its relationship with ER in epidermal cell development in the cotyledon. It is likely that by applying the same approach more genes functioning in epidermal development can be identified and even new aspects of known epidermal mutants may be revealed, which would significantly contribute to genetic studies of plant epidermal development.

The unique role of SUE in epidermal development

LRR-RKs are transmembrane kinases. Their known functions include binding signal peptides, conducting phosphorylation signal to downstream regulators, and eventually inhibiting the activity and stability of transcription factor SPCH (Zoulias *et al.*, 2018). Most of LRR-RKs or LRR-RLPs, such as ERL1 and 2 (Shapk *et al.*, 2005), TMM (Yang & Sack, 1995), and SERKs (Meng *et al.*, 2015), were reported to have negative effects on normal epidermal cells development and their mutations alter cell patterning. The function of SUE, however, is positive for epidermal cell production in the cotyledon, opposite to that of ER. In this regard, SUE and possibly At2G28990 are unique among the LRR-RKs that function in epidermal development.

The dosage effect of *sue-1* and *er-1* on epidermal cell production

The *ER/er-1 sue-1sue-1* mutants were generally similar to Col-0 in the cell numbers, and *er-1er-1 SUE/sue-1* mutants have significantly more epidermal cells than Ler (**Fig. 8B**). In an ascending manner of cell numbers: the copy number of the *er-1* allele and the *SUE* allele seem to be positively correlated with the epidermal cell number. (**Fig. 12**). When the heterozygosity of *ERECTA* was fixed, the epidermal cell numbers increased as the copy number of *SUE* increased. Inversely, when the heterozygosity of *SUE* was fixed, and the epidermal cell numbers increased as the copy of *er-1* increased. Therefore, the two loci appear to exhibit a dosage effect on epidermal cell production.
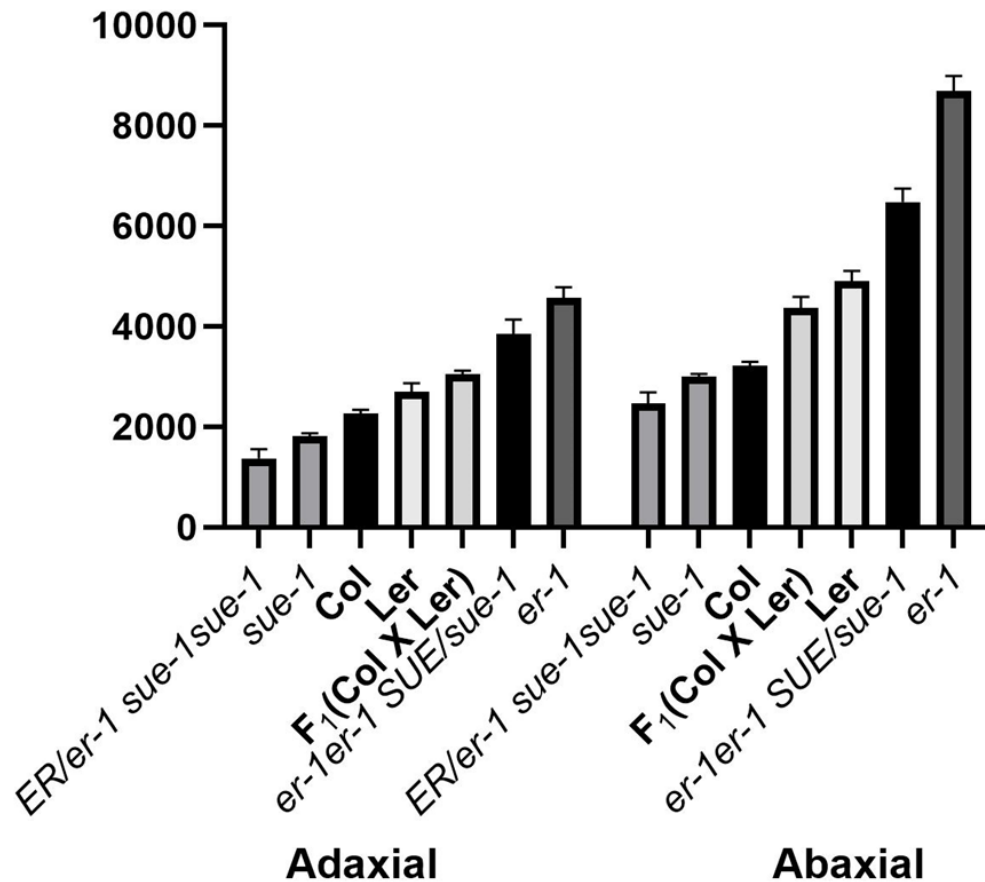
Fig. 12. Total cell numbers in plants of various genotypes. The cell numbers are arranged in an ascending order.

The suppressive effect of *sue* on trichomes

To further study the function of SUE in epidermal development and also guided by the *SUE:GUS* expression in trichomes, the number of trichomes on the first pair of leaves were counted. Both *er* mutants showed significantly fewer trichomes than Col (**Fig. 11**), which is consistent with the previous report (Marks & Esch, 1994). Both *sue* mutants also had significantly reduced trichomes compared to Col although *sue-2* appeared to have more trichomes than *sue-1*. Ler, the double mutant of *er-1 sue-1*, had the smallest number of trichomes while the *er-124 sue-2* double mutant was similar to the *er124* single mutant in the trichome number. The discrepancy between *sue-1* and *sue-2* or between Ler and *er-124 sue-2* may result from the presence of the *At2g28990* mutation in plants containing the *sue-1* mutation.

In trichome development, R_2R_3-MYB proteins have been found to play regulatory roles in trichomes initiation. These proteins include GL1 and MYB82, whose mutants produce glabrous or nearly glabrous leaves (Oppenheimer *et al.*, 1991; Liang *et al*., 2014). On the other hand, overexpression of *MYB23* causes the development of ectopic trichomes (Kirik *et al.*, 2001). Other R_2R_3-MYB genes such as *FOUR LIPS (FLP)* and *MYB88* have been identified as crucial genes for correct stomatal patterning (Lai *et al.*, 2005) and nonstomatal epidermal cells production (Yang, 2016).

The *SUE* gene found in this investigation plays a role in epidermal cell production, including the formation of stomatal lineages and trichomes. Further studies of the actions of SUE, ER, and possibly At2G28990 may shed light on how the LRR-RK pathway interacts with the R_2R_3-MYB pathway in epidermal development.

<div align="center">The relationship between SUE and ER</div>

Understanding the relationship between SUE and ER is important for developing a genetic network for the regulation of epidermal development. The *sue-1* mutant used in this investigation is expected to be the *sue-1 at2g28990* double mutant, which complicates the analysis of the relationship between SUE and ER. The *sue-2* mutant had slightly decreased or similar numbers of epidermal cells compared to Col-0 (**Fig. 10A**), but it caused relatively large reductions in the numbers of pavement cells and total epidermal cells in the adaxial epidermis in the *er-124 sue-2* double mutant when the double mutant is compared with *er-124* (**Table 2**). The numbers of pavement cells and total epidermal cells in the double mutant cannot be simply attributed to the combined effect of the single mutations. Based on these characteristics, the relationship between *er-124* and *sue-2* is neither additive nor epistatic. On the other hand, *er-124* and *sue-2* both had fewer trichomes than Col-0, and the trichome number in *er-124* was smaller than *sue-2* but about the same as that in *er-124 sue-2*, suggesting that *er-124* is epistatic to *sue-2* in trichome production (**Fig. 11**). These results together raise the possibility that SUE and ER may act at the same node in a genetic network for regulating epidermal cell production in Arabidopsis.

CHAPTER V

CONCLUSION

In this research, a novel LRR-RK gene, *SUE*, has been characterized as a suppressor of the *ER* gene in the development of epidermal cells. The *sue* mutations can partially suppress the abnormal increase in epidermal cells caused by the *er* mutations. An Ler-like epidermal phenotype was found as a result of the combined effect of *sue* and *er* mutations. The allelic combinations at the *SUE* and *ER* loci revealed a dosage effect on epidermal cell production. Both the *sue* and *er* mutations also reduced trichome numbers. The phenotypes of various genotypes suggest that that SUE and ER act at the same node of a genetic network. Moreover, At2G28990, the gene adjacent to *SUE* and encoding a SUE homolog was also implicated in the regulation of epidermal development involved. This research contributed to the comprehension of epidermal development and provided clues to future research in related areas.

REFERENCES

aan den Toorn, M., Albrecht, C., & de Vries, S. (2015). On the origin of SERKs: bioinformatics analysis of the somatic embryogenesis receptor kinases. *Mol. Plant, 8*(5), 762-782.

Abbruzzese, G., Beritognolo, I., Muleo, R., Piazzai, M., Sabatti, M., Mugnozza, G.S., & Kuzminsky, E. (2009). Leaf morphological plasticity and stomatal conductance in three Populus alba L. genotypes subjected to salt stress. *Environmental and Experimental Botany, 66*(3), 381-388.

Akita, K., Hasezawa, S., & Higaki, T. (2013). Breaking of Plant Stomatal One-Cell-Spacing Rule by Sugar Solution Immersion. *PLOS ONE 8*(9): e72456.

Bertolino, L. T., Caine, R. S., & Gray, J. E. (2019). Impact of Stomatal Density and Morphology on Water-Use Efficiency in a Changing World. *Frontiers in Plant Science, 10*, 225.

Bergmann, D.C., Lukowitz, W., & Somerville, C.R. (2004). Stomatal development and pattern controlled by a MAPKK kinase. *Science, 304*(5676), 1494-1497.

Blum, M., Chang, H., Chuguransky, S., Grego, T., Kandasaamy S., Mitchell, A., Nuka, G., Paysan-Lafosse, T., Qureshi, M., Raj, S., Richardson, L., Salazar, G.A., Williams, L., Bork, P., Bridge, A., Gough, J., Haft, D.H., Letunic, I., Marchler-Bauer, A., Mi, H., Natale, D.A., Necci, M., Orengo, C.A., Pandurangan, A.P., Rivoire, C., Sigrist, C.J.A., Sillitoe, I., Thanki, N., Thomas, P.D., Tosatto, S.C.E., Wu, C.H., Bateman, A. & Finn, R.D. (2020) The InterPro protein families and domains database: 20 years on. *Nucleic Acids Research*, *49*(D1), D344-D354.

Duan, Q., Kita, D., Li, C., Cheung, AY., & Wu, HM. (2010). FERONIA receptor-like kinase regulates RHO GTPase signaling of root hair development. *PNAS, 107*(41), 17821-17826.

Dong, J., MacAlister, C.A., & Bergmann, D.C. (2009). BASL Controls Asymmetric Cell Division in Arabidopsis. *Cell, 137*(7), 1320-1330.

Dong, Q., Zhuang, Z., Liu, Y., Tao, L.-Z., & Liu, H. (2019). FERONIA regulates auxin-mediated lateral root development and primary root gravitropism. *FEBS Letters, 593*, 97-106.

Franck, C.M., Westermann, J., & Boisson-Dernier, A. (2018). Plant Malectin-Like Receptor Kinases: From Cell WallIntegrity to Immunity and Beyond. *Annual Review of Plant Biology, 69*(1), 301-328.

Geisler, M., Nadeau, J., & Sack, F. D. (2000). Oriented Asymmetric Divisions That Generate the Stomatal Spacing Pattern in Arabidopsis Are Disrupted by the too many mouths Mutation. *The Plant Cell, 12*(11), 2075-2086.

Guo, X.-Y., Wang, Y., Xu, P., Yu, G.-H., Zhang, L.-Y., Xiong, Y., & Xiang, C.-B. (2017). AtEDT1/HDG11 regulates stomatal density and water-use efficiency via ERECTA and E2Fa. *New Phytologist, 223*(3), 1478-1488.

Gusman, J.M., Lee, J.S., Bogenschutz, N.L., Peterson, K.M., Virata, R.E., Xie, B., Kanaoka, M.M., Hong, Z., & Torii, K.U. (2010). Dysregulation of cell-to-cell connectivity and stomatal patterning by loss-of-function mutation in Arabidopsis CHORUS (GLUCAN SYNTHASE-LIKE 8). *Development 137*(10), 1731–1741.

Han, S., Tang, R., Anderson, L. K., Woerner, T. E., & Pei, Z. M. (2003). A cell surface receptor mediates extracellular Ca($2+$) sensing in guard cells. *Nature*, *425*(6954), 196–200.

Hara, K., Kajita, R., Torii, K. U., Bergmann, D. C., & Kakimoto, T. (2007). The secretory peptide gene EPF1 enforces the stomatal one-cell-spacing rule. *Genes & development, 21*(14), 1720-1725.

Haruta, M., Sabat, G., Stecher, K., Minkoff, BB., & Sussman, MR. (2014). A peptide hormone and its receptor protein kinase regulate palnt cell expansion. *Science, 343*(6169), 408-411.

He, K., Gou, X., Yuan, T., Lin, H., Asami, T., Yoshida, S., Russell, SD., Li, J. (2007). BAK1 and BKK1 regulate brassinosteroid-dependent growth and brassinosteroid-independent cell-death pathways. *Current Biology, 17*(13), 1109-1115.

Hetherington, A. M., & Woodward, F. I. (2003). The role of stomata in sensing and driving environmental change. *Nature, 424*(6951), 901-908.

Hunt, L., Bailey, K. J., & Gray, J. E. (2010). The signalling peptide EPFL9 is a positive regulator of stomatal development. *New Phytologist, 186*(3), 609-614.

Hunt, L., & Gray, J. E. (2009). The signaling peptide EPF2 controls asymmetric cell divisions during stomatal development. *Current Biology, 19*(10), 864-869.

Kim, T.W., Michniewicz, M., Bergmann, D.C., & Wang, Z.Y. (2012). Brassinosteroid regulates stomatal development by GSK3-mediated inhibition of a MAPK pathway. *Nature, 482*(7385), 419-422.

Kirik, V., Schnittger, A., Radchuk, V., Adler, K., Hülskamp, M., & Bäumlein, H. (2001). Ectopic expression of the Arabidopsis AtMYB23 gene induces differentiation of trichome cells. *Developmental biology*, *235*(2), 366–377.

Kollist, H., Nuhkat, M. & Roelfsema, M.R.G. (2014), Closing gaps: linking elements that control stomatal movement. *New Phytol, 203*(1), 44-62.

Lai, L. B., J. A. Nadeau, J. Lucas, E. K. Lee, T. Nakagawa, L. Zhao, M. Geisler, & F. D. Sack. (2005). The Arabidopsis R2R3 MYB proteins FOUR LIPS and MYB88 restrict divisions late in the stomatal cell lineage. *Plant Cell, 17*(10), 2754–2767

Lampard, G. R., Lukowitz, W., Ellis, B. E., & Bergmann, D. C. (2009). Novel and expanded roles for MAPK signaling in Arabidopsis stomatal cell fate revealed by cell type–specific manipulations. *The Plant Cell, 21*(11), 3506-3517.

Lampard, G. R., MacAlister, C. A., & Bergmann, D. C. (2008). Arabidopsis stomatal initiation is controlled by MAPK-mediated regulation of the bHLH SPEECHLESS. *Science, 322*(5904), 1113-1116.

Larkin, J. C., Marks, M. D., Nadeau, J., & Sack, F. (1997). Epidermal cell fate and patterning in leaves. *The Plant Cell, 9*(7), 1109-1120.

Lee, J. S., Hnilova, M., Maes, M., Lin, Y.-C. L., Putarjunan, A., Han, S.-K., Avila, J., & Torii, K. U. (2015). Competitive binding of antagonistic peptides fine-tunes stomatal patterning. *Nature, 522*(7557), 439-443.

Lee, J. S., Kuroha, T., Hnilova, M., Khatayevich, D., Kanaoka, M. M., McAbee, J. M., Sarikay, M., Tamerler, C., & Torii, K. U. (2012). Direct interaction of ligand-receptor pairs specifying stomatal patterning. *Genes & development, 26*(2), 126-136.

Li, J., Wen, J., Lease, K. A., Doke, J. T., Tax, F. E., & Walker, J. C. (2002). BAK1, an Arabidopsis LRR Receptor-like Protein Kinase, Interacts with BRI1 and Modulates Brassinosteroid Signaling. *Cell, 110*(2), 213-222.

Liang, G., He, H., Li, Y., Ai, Q., & Yu, D.Q., (2014). MYB82 functions in regulation of trichome development in Arabidopsis, *Journal of Experimental Botany, 65*(12), 3215-3223.

Lucas, J. R., Nadeau, J. A., & Sack, F. D. (2005). Microtubule arrays and Arabidopsis stomatal development. *Journal of Experimental Botany, 57*(1), 71-79.

MacAlister, C. A., Ohashi-Ito, K., & Bergmann, D. C. (2007). Transcription factor control of asymmetric cell divisions that establish the stomatal lineage. *Nature, 445*(7127), 537-540.

Marks, M.D., & Esch, J.J. (1994). Morphology and development of mutant and wild type trichomes on the leaves of Arabidopsis thaliana. *Arabidopsis: An atlas morphology and development*, 56-73.

Meng, X., Chen, X., Mang, H., Liu, C., Yu, X., Gao, X., Torii, K.U., He, P., & Shan, L. (2015). Differential function of Arabidopsis SERK family receptor-like kinases in stomatal patterning. *Current Biology, 25*(18), 2361-2372.

Merz, D., Richter, J., Gonneau, M., Sanchez-Rodriguez, C., Eder, T., Sormani, R., Martin, M., Hematy, K., Hofte, H., & Hauser, M.T. (2017). T-DNA alleles of the receptor kinase THESEUS1 with opposing effects on cell wall integrity signalling. *Journal of experimental botany, 68*(16), 4583-4593.

Nadeau, J.A., & Sack, F.D. (2002). Control of stomatal distribution on the Arabidopsis leaf surface. *Science, 296*(5573),1697-1700.

Ohashi-Ito, K., & Bergmann, D. C. (2006). Arabidopsis FAMA Controls the Final Proliferation/Differentiation Switch during Stomatal Development. *The Plant Cell, 18*(10), 2493-2505.

Oppenheimer, D. G., Herman, P. L., Sivakumaran, S., Esch, J., & Marks, M. D. (1991). A myb gene required for leaf trichome differentiation in Arabidopsis is expressed in stipules. *Cell, 67*(3), 483–493.

Papanatsiou, M., Amtmann, A., & Blatt, M. R. (2016). Stomatal Spacing Safeguards Stomatal Dynamics by Facilitating Guard Cell Ion Transport Independent of the Epidermal Solute Reservoir. *Plant Physiology, 172*(1), 254-263.

Pillitteri, L. J., Sloan, D. B., Bogenschutz, N. L., & Torii, K. U. (2007). Termination of asymmetric cell division and differentiation of stomata. *Nature, 445*(7127), 501-505.

Qi, X., & Torii, K.U. Hormonal and environmental signals guiding stomatal development. (2018) *BMC Biol 16*(1), 21.

Rédei, G. P. (1962). SUPERVITAL MUTANTS OF ARABIDOPSIS. *Genetics, 47*(4), 443-460.

Ryusuke, Y., Taku, T., Atsushi, K., Torii, K.U., & Yoshibumi, K. (1998). The Arabidopsis ERECTA gene is expressed in the shoot apical meristem and organ primordia. *The Plant Journal*, 15(3), 301-310.

Sachs, T. (1978). The development of spacing patterns in the leaf epidermis. In *The clonal basis of development* (pp. 161–183).

Shpak, E. D., Berthiaume, C. T., Hill, E. J., & Torii, K. U. (2004). Synergistic interaction of three ERECTA-family receptor-like kinases controls Arabidopsis organ growth and flower development by promoting cell proliferation. *Development, 131*(7), 1491-1501.

Shpak, E. D., McAbee, J. M., Pillitteri, L. J., & Torii, K. U. (2005). Stomatal Patterning and Differentiation by Synergistic Interactions of Receptor Kinases. *Science, 309*(5732), 290-293.

Sugano, S. S., Shimada, T., Imai, Y., Okawa, K., Tamai, A., Mori, M., & Hara-Nishimura, I. (2010). Stomagen positively regulates stomatal density in Arabidopsis. *Nature, 463*(7278), 241-244.

Tanaka, Y., Nose, T., Jikumaru, Y., & Kamiya Y. (2013). ABA inhibits entry into stomatal-lineage development in Arabidopsis leaves. *Plant J. 74*(3):448-457.

Tisné, S., Barbier, F., & Granier, C. (2011). The ERECTA gene controls spatial and temporal patterns of epidermal cell number and size in successive developing leaves of Arabidopsis thaliana. *Annals of botany, 108*(1), 159–168.

Torii, K. U. (2004). Leucine-rich repeat receptor kinases in plants: structure, function, and signal transduction pathways. *Int Rev Cytol, 234*(243), 1-46.

Torii, K. U., Mitsukawa, N., Oosumi, T., Matsuura, Y., Yokoyama, R., Whittier, R. F., & Komeda, Y. (1996). The Arabidopsis ERECTA gene encodes a putative receptor protein kinase with extracellular leucine-rich repeats. *The Plant Cell, 8*(4), 735-746.

von Groll, U., Berger, D., & Altmann, T. (2002). The Subtilisin-Like Serine Protease SDD1 Mediates Cell-to-Cell Signaling during Arabidopsis Stomatal Development. *The Plant Cell, 14*(7), 1527-1539.

Wang, W.-H., Chen, J., Liu, T.-W., Chen, J., Han, A.-D., Simon, M., Dong, X.-J., He, J.-X., & Zheng, H.-L. (2013). Regulation of the calcium-sensing receptor in both stomatal movement and photosynthetic electron transport is crucial for water use efficiency and drought tolerance in Arabidopsis. *Journal of Experimental Botany, 65*(1), 223-234.

Willmer C., F. M. (1996). *The distribution of stomata.*: Springer, Dordrecht.

Xie, C., Zhang, R., Qu, Y., Miao, Z., Zhang, Y., Shen, X., Wang, T., & Dong, J. (2012). Overexpression of MtCAS31 enhances drought tolerance in transgenic Arabidopsis by reducing stomatal density. *New Phytologist, 195*(1), 124-135.

Yang, M., & Sack, F.D. (1995). The too many mouths and four lips mutations affect stomatal production in Arabidopsis. *The Plant Cell, 7*(12), 2227–2239.

Yang, M. (2016). The FOUR LIPS (FLP) and MYB88 genes conditionally suppress the production of nonstomatal epidermal cells in Arabidopsis cotyledons. *American Journal of Botany, 103*, 1559-1566.

Yoo, C. Y., Pence, H. E., Jin, J. B., Miura, K., Gosney, M. J., Hasegawa, P. M., & Mickelbart, M. V. (2010). The Arabidopsis GTL1 Transcription Factor Regulates Water Use Efficiency and Drought Tolerance by Modulating Stomatal Density via Transrepression of SDD1. *The Plant Cell, 22*(12), 4128-4141.

Yu, H., Chen, X., Hong, Y.-Y., Wang, Y., Xu, P., Ke, S.-D., Liu, H.-Y., Zhu, J.-K., Oliver, D.J., & Xiang, C.-B. (2008). Activated Expression of an Arabidopsis HD-START Protein Confers Drought Tolerance with Improved Root System and Reduced Stomatal Density. *The Plant Cell, 20*(4), 1134-1151.

Zoulias, N., Harrison, E. L., Casson, S. A., & Gray, J. E. (2018). Molecular control of stomatal development. *The Biochemical journal, 475*(2), 441-454.

APPENDIX

Primer Sequences

In Set1 mutants, *SUE* and *sue* are amplified by 677+678, 705+684 respectively. In Set2 mutants, *SUE* and *sue* insertion amplified by 677+678, 677+LBa1 respectively; *ERECTA* and *erecta* insertion amplified by 703+704, 690+LBa1 respectively. The gel electrophoresis cannot distinguish *ERECTA* and *erecta*, the confirmation on this is based on sequencing.

LBa1: TGG TTC ACG TAG TGG GCC ATC G

677: GGA TCA TAG AGC CCG TCT TAC

678: GCT GGA GGA ATC AGA CCT TT

684: ATG CAT ATC AAG ACT GAA GTA G

690: CTT CTT GGG TTT CTC TTC TGC T

703: GTG GAG ATT GGA TTC GTC ATC A

704: CGA TTA AGC GGC TTT ACT CTT A

705: GGA GAT GGT GCA GTA GAG TTA TC

VITA

Xi Wen

Candidate for the Degree of

Master of Science

Thesis: REGULATION OF EPIDERMAL CELL PRODUCTION BY THE *SUPPRESSOR OF ERECTA* AND *ERECTA* GENES IN ARABIDOPSIS THALIANA

Major Field: Plant Biology

Biographical:

Education:

Completed the requirements for the Master of Science in Plant Biology at Oklahoma State University, Stillwater, Oklahoma in December 2021.

Completed the requirements for the Bachelor of Science in Agriculture at Shandong Agricultural University, Tai'an, China in June 2018.